Mol 2006/023564

# Experimental and modeling studies of desensitization of P2X₃ receptors

Elena Sokolova*, Andrei Skorinkin*, Igor Moiseev, Andrei Agrachev, Andrea Nistri, Rashid Giniatullin

Sectors of Neurobiology (ES, AS, AN, RG) and Functional Analysis (IM, AA), and CNR-INFM DEMOCRITOS National Simulation Center (ES, AN, RG), International School for Advanced Studies (SISSA), 34014 Trieste, Italy; Biochemical and Biophysical Institute of the Russian Academy of Sciences (AS), 420008 Kazan, Russia; Kazan Medical University (RG), 420012 Kazan, Russia.

**Running title page**


*Running title*: desensitization of P2X$_3$ receptors


*Abbreviations*: high affinity desensitization (HAD); trigeminal ganglia (TG); dorsal root ganglia (DRG); 2-Methylthioadenosine triphosphate tetrasodium salt (2-Me-SATP); cytidine 5′-triphosphate (CTP); 5-[[[(3-henoxyphenyl)methyl][(1S)-1,2,3,4-tetrahydro-1-naphthalenyl]amino]carbonyl]-1,2,4-benzenetricarboxylic acid sodium salt (A-317491).


Total length of MS: 37 pages, 6 Figures and 1 scheme, plus one supplemental material file.

Abstract: 250 words; Introduction: 317 words; Discussion: 1733 words.

All correspondence to: R. Giniatullin, SISSA, Via Beirut 4, 34104 Trieste, Italy; phone: 39-040-3787228; fax: 39-040-3787528; e-mail: rashid@sissa.it

## Abstract

The function of ATP-activated $P2X_3$ receptors involved in pain sensation is modulated by desensitization, a phenomenon poorly understood. The present study used patch-clamp recording from cultured rat or mouse sensory neurons and kinetic modelling to clarify the properties of $P2X_3$ receptor desensitization. Two types of desensitization were observed, a fast process ($t_{1/2}$=50 ms; 10 μM ATP) following the inward current evoked by micromolar agonist concentrations, and a slow process ($t_{1/2}$=35 s; 10 nM ATP) that inhibited receptors without activating them. We termed the latter high-affinity desensitization (HAD). Recovery from fast desensitization or HAD was slow and agonist-dependent. When comparing several agonists, there was analogous ranking order for agonist potency, rate of desensitization and HAD effectiveness, with 2-Me-SATP the strongest and β,γ-meATP the weakest. HAD was less developed with recombinant (ATP $IC_{50}$=390 nM) than native $P2X_3$ receptors ($IC_{50}$= 2.3 nM). HAD could also be induced by nanomolar ATP when receptors appeared to be non-desensitized, indicating that resting receptors could express high-affinity binding sites. Desensitization properties were well accounted for by a cyclic model in which receptors could be desensitized from either open or closed states. Recovery was assumed to be a multi-state process with distinct kinetics dependent on the agonist-dependent dissociation rate from desensitized receptors. Thus, the combination of agonist-specific mechanisms such as desensitization onset, HAD and resensitization could shape responsiveness of sensory neurons to $P2X_3$ receptor agonists. By using subthreshold

concentrations of an HAD-potent agonist, it might be possible to generate

sustained inhibition of $P2X_3$ receptors for controlling chronic pain.

## Introduction

ATP-activated P2X$_3$ receptors are expressed by sensory neurons to signal various forms of pain (North, 2002, 2004). One important property of such receptors is strong, long-lasting desensitization followed by full recovery (Cook et al., 1998, Sokolova et al., 2004). Unraveling the molecular mechanisms of this phenomenon can help to understand the basis of nociceptive transduction. In addition to very slow resensitization (Cook et al., 1998), our recent data (Sokolova et al., 2004) have demonstrated two novel features of P2X$_3$ receptors, namely agonist-specific recovery process and inactivation by sub-threshold concentrations (nanomolar) of agonist (see also Pratt et al., 2005). The latter phenomenon, termed high-affinity desensitization (HAD), had been initially described for muscle-type nicotinic receptors (Katz & Thesleff, 1957) and later shown with other nicotinic receptors (for review see Giniatullin et al., 2005). Because of the implication that ambient ATP levels (normally in the nanomolar range; Lazarowski et al., 2003) might control P2X$_3$ receptor activity, clarifying the exact mechanism of HAD should elucidate the issue of constitutive desensitization of P2X$_3$ receptors and their ability to respond to rapid changes in agonist concentrations. While one theory argues that high affinity binding sites responsible for HAD are available only when receptors are desensitized (Pratt et al., 2005), other studies suggest that even resting receptors express the HAD site (Rettinger & Schmalzing, 2003; Sokolova et al., 2004).

Kinetic modeling is an efficient tool to understand desensitization mechanisms of

ligand-gated receptors like GABA (Jones & Westbrook, 1995), AMPA (Bowie & Lange, 2002), or certain subtypes of P2X receptors such as $P2X_1$ (Rettinger and Schmalzing, 2003) or $P2X_2$ receptors (Ding and Sachs, 1999; Skorinkin et al., 2003). Nevertheless, there are no kinetic models of $P2X_3$ receptors.

In the present study, using cultured mouse or rat sensory neurons, we experimentally investigated the main desensitization properties of native $P2X_3$ receptors and generated, for the first time, a receptor model to simulate their behavior during different conditions.

## Materials and Methods

### Cell cultures

Rat or mouse trigeminal (TG) or dorsal root ganglion (DRG) neurons in culture were prepared as previously described (Sokolova et al., 2001; Simonetti et al., submitted). Animals (2-3 week old) of both sexes were deeply anesthetized with ether and killed by decapitation, a procedure (including animal handling and care) in accordance with the Italian Animal Welfare Act and approved by the Local Authority Veterinary Service. Such a procedure accords with the European Communities Council Directive (24th November 1986; 86/609/EEC). Neurons were plated on poly-*l*-lysine (5 mg/ml) coated Petri dishes and cultured for 1-2 days under an atmosphere containing 5 % $CO_2$. Nerve growth factor (2.5S NGF; 50 ng/ml) was added at the time when DRG neurons were attached to poly-*l*-lysine. TG neurons were grown without adding NGF. Cells were used within 2

days of plating when they lacked processes.

HEK-293T cells prepared as previously reported (Sokolova et al 2004; Fabbretti et al 2004) and transfected with the $rP2X_3$ gene kindly provided by Prof. R.A. North (University of Manchester).

### Electrophysiological recording

Cells (15-30 μm diameter) were recorded in the whole cell configuration while continuously superfused with control solution containing (in mM): NaCl 152, KCl 5, $MgCl_2$ 1, $CaCl_2$ 2, glucose 10, HEPES 10; pH was adjusted to 7.4 with NaOH and osmolarity was adjusted to 320 mOsm with glucose. To compare the present data with those reported by Pratt et al. (2006), we also performed experiments using the following extracellular solution (mM): NaCl 135, KCl 5, $CaCl_2$ 1, $MgCl_2$ 2, HEPES 10 and glucose 10 (287 mOsm).

Patch pipettes had a resistance of 3-4 MΩ when filled (in mM) with CsCl 130; HEPES 20; $MgCl_2$ 1, magnesium ATP 3; EGTA 5; pH was adjusted to 7.2 with CsOH. Osmolarity of the pipette solution was adjusted to 290 mOsm with sucrose. In a series of experiments the pipette solution included, instead of CsCl, KCl (130 mM) and EGTA was raised to 10 mM. Since there was no detectable difference in $P2X_3$ receptor mediated responses, data were pooled for analysis. To enable comparison of our results with data by Pratt et al. (2005), we also run experiments using a pipette solution comprising (mM) KCl 55, $K_2SO_4$ 60, $MgCl_2$ 7, EGTA 10, HEPES 10 (pH adjusted with KOH). In most cells series resistance was compensated by 80 %. Cells were voltage-clamped at -70 mV. Currents

were filtered at 1 kHz and acquired on IBM PC by means of pCLAMP 7.0 software (Axon Instruments, Foster City, CA).

### *Drug delivery*

Agonists and antagonists were applied (usually for 2 s) via a rapid superfusion system (Rapid Solution Changer RSC-200, BioLogic Science Instruments, Grenoble, France) placed 100-150 μm near the cell. Time for the solution exchange across the cell was about 30 ms as judged with liquid junction potential measurements.

All chemicals, including enzymes for cell culture, were from Sigma (Milan, Italy); culture mediums were obtained from Gibco BRL (Life Technologies, Milan, Italy). The following ATP receptor agonists were used: 2-Me-SATP, ATP, $\alpha,\beta$-meATP, $\beta,\gamma$-meATP.

### *Data analysis*

In accordance with previous studies (Krishtal et al., 1988; Burgard et al., 1999; Grubb and Evans, 1999) $P2X_3$ receptor-mediated responses induced by maximally-effective concentrations of agonist were observed as fast (20-80 % onset time <60 ms) inward currents with full desensitization during a 2 s pulse application. These responses were measured in terms of their peak amplitude using pCLAMP software (ClampFit version 9). For each agonist, dose response plots were constructed by normalizing data with respect to the maximum one. All data are presented as mean±s.e.mean (n = number of cells) with statistical

significance assessed with paired $t$-test (for parametric data) or Mann-Whitney

rank sum test (for non-parametric data). Best fits of data with a sigmoid function

were compared with respective control fits using Origin software (version 6.0). A

value of p<0.05 was accepted as indicative of statistically significant difference.

The fitting function for recovery (R) as a function of time (t) was in the form of the

Boltzmann equation:

$$R(t) = \frac{A_1 - A_2}{1 + e^{\frac{t - t_o}{dt}}} + A_2 \tag{eq. 1}$$

where $A_1$, $A_2$, are the start and finish levels.


### Computer simulation method

In general, our approach to modeling has been recently described as far as $P2X_2$

receptors were concerned (Skorinkin et al., 2003) and is based on a set of

differential equations with the probability of occurrence of each receptor state

given by:

$$\frac{d\overline{P}(t)}{dt} = \mathbf{Q} \cdot \overline{P}(t) \tag{eq. 2}$$

where $\overline{P}$ is a vector composed of probabilities of the receptor occupying each

kinetic state at time t, and Q is the matrix of transitions between the states. Our

in-house-developed program was written in Pascal and used on an IBM-

compatible PC to solve numerically this set of differential equations using the

eight-order Runge-Kutta method (Baker et al., 1996).

### *Selecting a kinetic model accounting for desensitization of P2X₃ receptors*

**Step-1.** In order to develop a kinetic model of the $P2X_3$ receptor in which desensitization played a major role, we first examined how the sigmoidal time-dependence of recovery from desensitization could point us toward certain basic features of agonist/receptor interaction. By assuming a set of linear reactions leading to various receptor states in which each transition step is independent (Bowie and Lange, 2002), we constructed a series of theoretical curves (plotting the extent of recovery versus time on linear scales) with different degree of sigmoidicity depending on the number of states. The mathematical approach used to construct these curves is described in supplemental file #1. Each curve is identified by its inflection point expressed as % of the full recovery (**Supplemental Fig 1).** This figure shows that increasing the number of states was associated with a rightward shift of the curve inflection point, starting from the simplest case of one reaction step (two states only described by standard hyperbole). Recovery became very slow with a large number of states, while the value of the inflection point moved within two relatively narrow boundaries. These observations collectively suggested that the sigmoidal timecourse of the ATP recovery from desensitization should be based on a multi-reaction process, a notion which accords with the stoichiometry of 3 molecules of ATP bound to a single receptor (Nicke et al., 1998; North, 2002).

**Step-2.** We next examined whether existing kinetic models derived for other ionotropic receptors (Jones and Westbrook, 1996) could be applicable to the $P2X_3$ receptor. There are at least three main reaction schemes: 1) the sequential

one used, for example, for P2X$_1$ receptors (Rettinger and Schmalzing, 2003); 2) the bifurcation scheme widely used to describe desensitization of GABA$_A$ receptors (Jones and Westbrook, 1996); 3) the cyclic scheme for acetylcholine receptors (Katz and Thesleff, 1957; Paradiso and Steinbach, 2003; Giniatullin et al., 2005). We used the following simple criteria for initial screening of a model: a) ability to simulate ATP currents with appropriate timecourse including full desensitization; b) slow recovery with sigmoidal timecourse. With such requirements, supplemental Fig 2 shows that neither the sequential (B) nor the bifurcation (C) model could replicate the sigmoidal recovery typical of fast, full current desensitization (experimental data are shown in A). These observations confirm that the process responsible for a sigmoidal recovery curve of P2X$_3$ receptors requires distinct reaction pathways for desensitization onset and recovery in analogy to other ionotropic receptors (Patneau and Mayer, 1991; Jonas, 1993; Raman and Trussell, 1995). Because the cyclic model contains such a feature, we considered whether it might be appropriate to simulate P2X$_3$ receptor operation.

**Step-3.** As previously suggested (Sokolova et al., 2004; Pratt et al., 2005), we assumed that the agonist dissociation from receptors (rather than agonist-independent receptor isomerization from the desensitized-unbound state D to the resting state R) was a rate limiting step in the recovery process from desensitization. Since the fastest recovery from experimental desensitization has 0.25 s$^{-1}$ rate (Pratt et al., 2005), we took this rate constant to be the upper limit for the D to R transition.

**Step-4**. Assuming that desensitization could develop from closed receptors without their activation (see Results), it was possible to devise a cyclic model as shown in Scheme 1.

**Step-5**. Once this kinetic scheme for desensitization was found to be appropriate, it was necessary to refine the model for adequate simulation of experimental results such as: i) dose-peak current curve; ii) dose-dependence of current decay; iii) recovery from desensitization; iv) HAD; v) effect of early or late agonist application for obtaining the rate constants for receptor activation and desensitization. The rate constants of the cyclic model were found from the best fit of experimental results and are listed for various agonists in supplemental Table 1. With this notation, standard desensitization was assumed to develop from open, bound channels only (A3R°), while HAD was supposed to originate mainly from the AR to AD reaction (with very small contribution from A2D and A3D states).

**Results**

***Comparison of desensitization properties of several P2X$_3$ agonists***

Fig 1 A shows an example of inward currents activated by several P2X$_3$ agonists such as β,γ-meATP, α,β-meATP, ATP or 2-Me-SATP (each at 10 µM) applied to the same DRG neuron. Responses peaked and decayed back to baseline within 2 s, indicating complete receptor desensitization. Fig 1 B shows dose response curves for these four agonists (n=5-10 cells) that enabled calculating the

following order of potency: 2-Me-SATP ($EC_{50}$=0.29 μM) > ATP ($EC_{50}$=1.5 μM) ≥

α,β-meATP ($EC_{50}$=1.8 μM) > β,γ-meATP ($EC_{50}$=18 μM). All these agonists

produced equivalent maximum responses. The current decay, which represents

the onset of desensitization, when tested with 10 μM agonist concentration, was

similarly fast (half decay time=0.06±0.01 s, 0.06±0.01 s, 0.06±0.02 s,

respectively) for 2-Me-SATP, ATP and α,β-meATP, while it was 3-time slower for

β,γ-meATP (Fig 1 C).  Conversely, there was no homogeneity for current decay

at lower agonist concentrations (Fig. 1 C), suggesting that different agonists

demonstrated distinct abilities to generate desensitization (Fig 1 C). Fig 1 A

shows such an example, namely that the time-course of the current evoked by 1

μM β,γ-meATP decayed much slower than the one elicited by the other agonists.

Recovery from desensitization (explored by paired-pulse protocol; Sokolova et

al., 2004) and expressed as $t_{1/2}$ (time to regain 50 % of control peak amplitude)

was also agonist-specific since it was very slow ($t_{1/2}$=3.22±0.07 min, n=7) for 2-

Me-SATP and very fast ($t_{1/2}$= 0.32±0.03 min, n=5) in the case of β,γ-meATP (Fig

2). The recovery curve for equi-effective concentrations of 2-Me-SATP (1 μM),

ATP (10 μM) or α,β,-meATP (10 μM) was best fitted by a sigmoidal function.

All agonists tested at maximal concentrations demonstrated complete cross-

desensitization, indicating that they activated the same receptor class (Sokolova

et al., 2004) blocked by the selective antagonist A-317491 (1 μM; see

supplemental Fig. 3).

Thus, both desensitization onset and resensitization were agonist-specific

phenomena varying from very prompt regain of function (β,γ-meATP) to

exceptionally slow one (2-Me-SATP).

### Desensitization by low concentrations of agonists

We previously demonstrated that HAD could develop after low agonist concentrations that did not evoke macroscopic receptor activation (Sokolova et al., 2004). To further explore HAD properties, we employed the same protocol whereby 6 min after a first test pulse of 10 $\mu$M ATP (test$_1$), a conditioning, small dose of an agonist was applied for varying length of time, and the sensitivity of P2X$_3$ receptors tested again with a second pulse of 10 $\mu$M ATP (test$_2$). While 10 nM $\alpha,\beta$-meATP induced a moderate, depressant effect (compare top and bottom traces in Fig 3 A), the same concentration of 2-Me-SATP was much more effective to inhibit test responses (see top and bottom traces in Fig 3 B). Fig 3 C shows that the HAD produced by 10 nM ATP was time-dependent and reached an apparent maximum near 90 s (decay time constant = 37.1± 4.0 s; n=4-7). This application time was then used for comparative purposes with various agonists as indicated in Fig. 3 D that shows how the HAD order of potency ranged from 2-Me-SATP (IC$_{50}$=0.26 nM), followed by ATP (IC$_{50}$= 2.3 nM), $\alpha,\beta$-meATP (IC$_{50}$= 20 nM), and $\beta,\gamma$-meATP (IC$_{50}$ = 570 nM). This ranking order was therefore similar to the agonist potency (2-Me-SATP >ATP>$\cong\alpha,\beta$-meATP>$\beta,\gamma$-meATP; Fig. 1 B). Comparison between potency and HAD for each agonist is illustrated in Supplemental Fig 4 A. Recombinant rP2X$_3$ receptors expressed by HEK293T cells tested with ATP pulses, showed less HAD (IC$_{50}$ = 390 nM) than native ones (Supplemental Fig 4 B).

In general, our results demonstrated slow development and agonist-specific property of HAD. Amongst the tested agonists, 2-Me-SATP was the most effective one to produce HAD.

### *Mechanism of HAD*

There are at least two mechanisms to account for HAD. One implies low concentrations of agonist binding to desensitized receptors only, with consequent retardation of their recovery (Pratt et al., 2005). An alternative process, which may be inferred from $P2X_1$ receptors (Rettinger and Schmalzing, 2003), assumes that resting receptors already express high affinity binding sites capable of entering into desensitized state.

Using a protocol similar to one suggested by Pratt et al., (2005), we took advantage from the fact that recovery from $\beta,\gamma$-meATP-induced desensitization is much faster than from desensitization induced by ATP. On mouse TG neurons, using paired applications of 100 $\mu$M $\beta,\gamma$-meATP separated by 120 s intervals (test$_1$ and test$_2$, respectively), we applied 10 nM ATP either for 60 s immediately after test$_1$ (early conditioning) or for 60 s preceding the test$_2$ (late conditioning). Early conditioning produced strong HAD (mouse: 73±6 % inhibition, n=6; P<0.01; rat: 77±4 % inhibition, n=6; P<0.01; Fig. 4 A,C) as expected (Pratt et al., 2005). It should, however, be noted that even late conditioning (when 10 nM ATP was applied to recovered receptors) produced significant HAD (mouse: 42±8 % inhibition, n=6; P<0.05; rat: 49±5 % inhibition, n=6; P<0.05; Fig. 4 B,D) followed by slow recovery (Fig. 4 B).

We also checked the ability to induce HAD by 10 nM ATP (30 s application) when the test pulses were evoked by relatively small concentrations of $\beta,\gamma$-meATP (3 $\mu$M) to produce responses with limited receptor activation (see top left trace in Fig. 4 E). Both 'early' (immediately after first test pulse of $\beta,\gamma$-meATP) or 'late' (following 30 s wash period after $\beta,\gamma$-meATP first test) applications of 10 nM ATP produced a very similar degree of depression (Fig 4 F).

One noticeable difference between the present experiments and those by Pratt et al. (2005) is the composition of the intra and extracellular solutions. We therefore performed a number of experiments on rat DRG neurons to check whether, by running our experiments with the same solutions used by Pratt et al (2005), analogous data could be obtained. First, we measured the recovery time from desensitizing test pulses of $\beta,\gamma$-meATP (100 $\mu$M) in the Pratt's solution: supplemental Fig 4 C shows that, in this case, recovery was slower than in the presence of our standard solution. In particular, one min after the test pulse of $\beta,\gamma$-meATP, recovery was incomplete (83±4 %, n=8). Supplemental Fig D indicates that HAD produced by 10 nM ATP application (60 s) on test$_2$ pulses of $\beta,\gamma$-meATP was the same when nanomolar ATP was applied immediately after the test$_1$ pulse (83±7 % inhibition, n=8) or 60 s prior to test$_2$ pulse (84±8 % inhibition; n=8).

These data showed the development of HAD by nanomolar ATP, regardless of receptor occupancy, and arising even when receptors had recovered from desensitization tested in the presence of different experimental solutions.

### *A general model for P2X$_3$ receptor operation*

As indicated in supplemental Fig. 2, traditional receptor models based on sequential activation and desensitization of receptors, or on a gateway scheme (with bifurcation of reactions between activation or desensitization states), could not replicate our experimental observations. Thus, we selected a kinetic model (see Methods) that could replicate the experimental features of P2X$_3$ receptor-mediated responses. Fig. 5 A (inset) shows that our model adequately simulated all the characteristics (rapid onset, peak and decay) of the ATP-evoked current. Furthermore, theoretical dose-response curves obtained with this model closely fitted experimental data points (compare Fig. 5 A with Fig. 1 B). Fig. 5B illustrates model-based simulation of the dissimilar current decay for various agonists in accordance with experimental data of Fig. 1 C, while agonist-specific, sigmoidal timecourse of recovery is shown in Fig. 5 C in good agreement with data of Fig. 2.

Fig. 5 D shows the differential inhibitory action produced by various conditioning agonists applied at various concentrations for 90 s prior to test responses evoked by 10 µM ATP: these plots are in close accordance with the experimental data of Fig. 3 D. Finally, the model reproduced the dissimilar depression by early (Fig. 5 E) or late (Fig. 5 F) application of 10 nM ATP on test β,γ-meATP pulses (see experimental results in Fig 4 C,D). Overall, the good approximation of simulated properties produced with the present model suggested it to be adequate to describe P2X$_3$ receptor kinetics.

**Influence of HAD on ATP-induced currents**

It was interesting to explore if, assuming that ambient ATP was subthreshold to produce HAD, HAD itself could be generated during pulse application of ATP and limit the amplitude and duration of the observed current. Because, in practice, it would be difficult to ensure zero concentration of ATP, by modeling it was feasible to simulate conditions of no ambient ATP and to test if HAD developing during a single pulse application of ATP could actually limit the agonist response. Thus, we simulated the receptor behavior when there was no HAD (by assuming a very low probability of transition from AR to AD states) and compared it with standard conditions. Fig. 6 shows that presence or absence of HAD did not change the peak amplitude of responses to half-maximal (1 μM) or near-threshold (100 nM) concentration of ATP. Nevertheless, HAD shortened current decay after 100 nM rather than 1 μM ATP, as in the latter case the current declined mainly via desensitization originating from open channels. The simulation predicts that HAD would mainly play a long-lasting modulatory role on the ability of receptors to signal, while conventional desensitization can play a major role in shaping fast currents evoked by ATP.

**Discussion**

The present study provides the first, kinetic model-based description of the desensitization properties of P2X$_3$ receptors. In addition to fast desensitization, P2X$_3$ receptors could undergo HAD developing without prior receptor activation

(Pratt et al., 2005, Sokolova et al., 2004). While HAD was induced by nanomolar concentrations of agonist, the current investigation suggests that this process even occurred via direct transition of receptors from their closed states to inactive ones.


### $P2X_3$ receptor properties

On DRG or TG neurons fast responses mediated by ATP or related analogues were due to activation of $P2X_3$ receptors because of their sensitivity to the selective blocker A-319471 (Jarvis et al., 2002) and full cross-desensitization between agonists. Furthermore, similar responses were observed with the HEK293T expressed $P2X_3$ receptors. Inward currents generated by near-maximal concentrations of agonists rapidly faded back to baseline indicating fast desensitization (Krishtal et al., 1988; Burgard et al., 1999; Grubb and Evans, 1999) with slow recovery (Cook et al., 1998; Giniatullin et al., 2003). Recovery from desensitization (resensitization) is characterized by sigmoidal time course (Sokolova et al., 2004) in accordance with a multistep process dependent on the nature of the agonist used (Sokolova et al., 2004; Pratt et al., 2005). It is noteworthy that, for comparable receptor activation, the rate of development of desensitization also depended on the agonist, indicating differential ability to enter into desensitized states. Note that with 2-Me-SATP, desensitization (including HAD) was particularly strong and recovery very delayed.

Interestingly, there was a similar ranking order of agonist potency, onset of desensitization and effectiveness to evoke HAD, suggesting that all these

different phenomena could be explained via the intrinsic properties of each agonist operating on the same class of receptor, rather than assuming a role for external factors like intracellular or metabolic changes (Gerevich et al., 2005).

### HAD: agonist-related properties

A subtle method to modulate receptors would be to condition them with agonist concentrations per se subthreshold to elicit detectable currents. Such an approach is interesting for two reasons: it might indicate that $P2X_3$ receptors are constitutively modulated by ambient ATP (and related purines; Cook et al., 1998), and that sustained block of $P2X_3$ receptors might be achieved by using a subthreshold agonist dose rather than an antagonist.

Although previous studies have reported HAD of $P2X_3$ receptors (Sokolova et al., 2004, Pratt et al., 2005), it was not clear whether receptors should be first desensitized to observe this phenomenon or whether naïve receptors can generate it. This issue is not trivial because it has distinct functional implications: first, one might expect HAD to intensify and prolong the inhibition of receptors after exposure to a high dose of agonist as occurring during synaptic transmission or pathophysiological conditions. Second, one would predict that receptors are constitutively subjected to a degree of inhibition which depends primarily on the ambient level of ATP. In molecular terms, these interpretations presume high affinity binding sites expressed by either desensitized or resting receptors.

One important observation emerging from the present study was that the extent

of HAD depended on the agonist exposure time. With the natural agonist ATP (10 nM), exposure <90 s could not produce full HAD. It is also interesting that HAD was not dependent on the fraction of receptors activated by agonist test pulses because it equally affected very low-amplitude responses generated by small doses of $\beta,\gamma$-meATP. Hence, the observed discrepancy in the intensity of HAD between native and recombinant $P2X_3$ receptors (despite analogous agonist potency; North, 2002; Fabbretti et al., 2004) might not be simply due to a dissimilar number of activated receptors and might imply some post-translational receptor change by the host cell.

Despite similar $EC_{50}$ value for ATP and $\alpha,\beta$-meATP, their $IC_{50}$ value for HAD was very different, suggesting that differential HAD inducing properties did not simply originate from dissimilar receptor activating abilities.

The present results accord with the former description of the "metaphilic effect" of an agonist that could produce a long-lasting change in receptor affinity to another agonist (Rang and Ritter, 1969). This phenomenon, extensively investigated with nicotinic receptors, had suggested a sustained molecular change of the receptor following initial exposure to the agonist and was interpreted as due to desensitization (Rang and Ritter, 1970a,b) because certain agonists that were very effective to desensitize receptors, were also the most powerful to produce a metaphilic effect. In the framework of this interpretation, the HAD evoked by nanomolar ATP may therefore be considered as a metaphilic effect. Rang and Ritter's interpretation derived from studying nicotinic receptors, cannot, however, be extended to all aspects of the dynamics of $P2X_3$ receptor desensitization,

because these authors reported agonist-independent recovery from desensitization progressing at a standard rate (Rang and Ritter, 1970a,b), properties clearly different from those typical of P2X$_3$ receptors.

### HAD: a memory process for receptor signaling?

When subthreshold agonist concentrations were applied immediately after a desensitizing dose of agonist, the subsequent test responses were strongly depressed in accordance with previous studies (Pratt et al., 2005). Recovery of test responses was delayed in the order of several minutes. Nevertheless, when the conditioning nanomolar agonist was applied after a time sufficient for recovery from desensitization, the subsequent test response was also decreased, though quantitatively less than with the protocol of early application. This phenomenon could be most conveniently observed by using $\beta,\gamma$-meATP as test agonist to produce responses characterized by fast recovery. Because significant HAD (~40-50 % depending on mouse or rat neurons) was induced by late application of 10 nM ATP, it is suggested that HAD could also occur in the virtual absence of preceding desensitization.

There are several reasons why this phenomenon was not reported before (Pratt et al., 2005). One might be the use of recombinant P2X$_3$ receptors which, as shown in the present study, displayed less HAD. Another is that full development of HAD required a relatively long time (at least 90 s), whereas previous investigations had been based on partially-developed HAD. Third, the experimental solutions used by Pratt et al (2005) contained lower extracellular

$Ca^{2+}$ and higher $Mg^{2+}$ concentrations than the ones used by us. Since it was shown that the ratio of these divalent cations is very important to control the process of recovery from desensitization of P2X$_3$ receptors (Giniatullin et al., 2003), it seemed feasible that discrepancies between studies could have been accounted by the actual degree of receptor desensitization. Indeed, when using Pratt's solution, we could observe slowdown of recovery. Nevertheless, HAD could be readily demonstrated with early and late application of nanomolar ATP. Finally, human P2X$_3$ receptors that were mainly investigated by Pratt et al. (2005) may possess kinetic properties different from rat or mouse ones. Some of these factors could have contributed to explain the observed differences.

In summary, we propose that HAD induced by nanomolar agonist doses contributed to inhibition of P2X$_3$ receptors via two processes, namely slowing of resensitization, and facilitation of the transition from close-bound receptor to desensitized state.

### *Cyclic model of P2X$_3$ receptor function can explain P2X$_3$ receptor desensitization*

To date, studies of P2X$_3$ receptor function lacked a kinetic model to account for their behavior. To build one, we excluded sequential or bifurcation schemes as shown in Supplemental Fig. 2, because we could not replicate fast currents with slow, sigmoidal time course of recovery from desensitization. Mathematical solutions indicated complex mechanisms for the recovery process that suggested a cyclic model of receptor operation implying multiple, interconnected states. This

cyclic model resembles those currently in use for describing nicotinic ACh receptors (Paradiso and Steinbach, 2003; Giniatullin et al., 2005) or AMPA receptors (Bowie and Lange, 2002). The model assumed that, for full receptor activation, agonist molecules must occupy three binding sites (Nicke et al., 1998; North, 2002) from which they would dissociate sequentially. After optimization, the cyclic scheme met multiple criteria including closely-reproduced fast currents with complete desensitization, slow recovery with sigmoidal timecourse, agonist dependent rate of recovery, agonist dose-response curves, and differential agonist potency to induce HAD, and HAD differences dependent on early or late agonist application.

In accordance with previous experimental suggestions (Sokolova et al., 2004), the present receptor model predicts that the major difference between ATP and other analogues could be attributed to the rate of agonist dissociation from multiple desensitized receptors. Relatively slow desensitization, rapid recovery and modest HAD could then reflect the property of a certain drug (like $\beta,\gamma$-meATP) to unbind quickly from desensitized receptors. This proposal is reminiscent of the properties of nicotinic receptors also displaying agonist-dependent recovery from desensitization (Reitstetter et al., 1999) attributed to differential dissociation rate constants (Mike et al., 2000). Furthermore, slow agonist dissociation is also thought to limit recovery of $P2X_1$ receptors (Rettinger & Schmalzing, 2003). Our model could not produce a sigmoidal recovery timecourse (data not shown), when we assumed that only desensitized receptors could be converted to resting ones via a simple, two-step transition (Pratt et al.,

2005).

It is generally difficult to demonstrate experimentally whether a certain degree of HAD is inevitably associated with responses even in the absence of ambient ATP. Our model enabled us to simulate responses after minimizing the HAD process, and predicted that the role of HAD was to control the current decay after small doses of ATP. Peak amplitude was apparently unaffected by HAD.

### *Functional implications*

Because nanomolar concentrations of endogenous ATP are normally found in the extracellular space (Phillis et al., 1993; Kuzmin et al., 1998; Nishiyama et al., 2000; He et al. 2005), a significant fraction of $P2X_3$ receptors on nociceptive sensory neurons in vivo should be desensitized and thus unable to sense changes in ATP concentrations produced after acute tissue damage (Cook and McCleskey, 2002). This hypothesis accords with the relatively-preserved acute pain perceived by $P2X_3$ knockout mice (Cockayne et al., 2000; Souslova et al., 2000). Nevertheless, there is strong evidence for a role of $P2X_3$ receptors in neuropathic and chronic pain (Cockayne et al., 2000; Souslova et al., 2000; Burnstock, 2001; Jacobson et al., 2002) in which plastic changes in the structure and function of $P2X_3$ receptors is supposed to occur (North, 2004). Our study shows that the HAD may be a process for limiting the function of $P2X_3$ receptors. Since HAD is agonist-specific, it might be possible in future to devise novel agonists with stronger HAD properties to control chronic pain states.

**REFERENCES**:

Baker TS, Dormand JR, Gilmore JP and Prince PJ (1996) Continuous approximation with embedded Runge-Kutta methods. *Appl Numl Math* **22**:51–62.

Bowie D and Lange GD (2002) Functional stoichiometry of glutamate receptor desensitization. *J Neurosci* **22**: 3392-3403.

Burgard EC, Niforatos W, Van Beissen T, Lynch KJ., Touma E, Metzger RE, Kowaluk EA and Jarvis MF (1999) P2X receptor-mediated ionic currents in dorsal root ganglion neurons. *J Neurophysiol* **82**: 1590-1598.

Burnstock G (2001) Purine-mediated signalling in pain and visceral perception. *Trends Pharmacol Sci* **22**:182-188.

Cockayne DA, Hamilton SG, Zhu QM, Dunn PM, Zhong Y, Novakovic S, Malmberg AB, Cain G, Berson A, Kassotakis I, Hedley I, Lachnit WG, Burnstock G, McMahon SB and Ford AP (2000) Urinary bladder hyporeflexia and reduced pain-related behaviour in P2X$_3$-deficient mice. *Nature* **407**: 951-952.

Cook SP and McCleskey EW (2002) Cell damage excites nociceptors through release of cytosolic ATP. *Pain* **95**: 41-47.

Cook SP, Rodland KD and McCleskey EW (1998) A memory for extracellular Ca$^{2+}$ by speeding recovery of P2X receptors from desensitization. *J Neurosci* **18**: 9238-9244.

Ding S and Sachs F (1999) Single channel properties of P2X$_2$ purinoceptors. *J Gen Physiol* **113**: 695-720.

Gerevich Z, Muller C and Illes P (2005) Metabotropic P2Y$_1$ receptors inhibit P2X$_3$ receptor-channels in rat dorsal root ganglion neurons *Eur J Pharmacol* **521**:34-38.

Giniatullin R, Sokolova E and Nistri A (2003) Modulation of P2X$_3$ receptors by Mg$^{2+}$ on rat DRG neurons in culture. *Neuropharmacology* **44**: 132-140.

Giniatullin R, Nistri A and Yakel JL (2005) Desensitization of nicotinic ACh receptors: shaping cholinergic signaling *Trends Neurosci* **28**:371-378.

Grubb BD and Evans RJ (1999) Characterization of cultured dorsal root ganglion neuron P2X receptors. *Eur J Neurosci* **11**: 149-154.

Fabbretti E, Sokolova E, Masten L, D'Arco M, Fabbro A, Nistri A, Giniatullin R (2004) Identification of negative residues in the P2X$_3$ ATP receptor ectodomain as structural determinants for desensitization and the Ca$^{2+}$-sensing modulatory sites. *J Biol Chem* **279**: 53109-53115.

He M-L, Gonzalez-Iglesias AE, Tomic M and Stojilkovic SS (2005) Release and extracellular metabolism of ATP by ecto-nucleotidase eNTPDase 1–3 in hypothalamic and pituitary cells. *Purinergic Signalling* **1**:135-144.

Jacobson KA, Jarvis MF and Williams M (2002) Purine and pyrimidine (P2) receptors as drug targets. *J Med Chem* **45**: 4057-4093.

Jarvis MF, Burgard EC, McGaraughty S, Honore P, Lynch K, Brennan TJ, Subieta A, Van Biesen T, Cartmell J, Bianchi B, Niforatos W, Kage K, Yu H, Mikusa J, Wismer CT, Zhu CZ, Chu K, Lee CH, Stewart AO, Polakowski J,

Cox BF, Kowaluk E, Williams M, Sullivan J, Faltynek C (2002) A-317491, a novel potent and selective non-nucleotide antagonist of P2X$_3$ and P2X$_{2/3}$ receptors, reduces chronic inflammatory and neuropathic pain in the rat. *Proc Natl Acad Sci USA* **99**:17179-17184.

Jonas P (1993) AMPA-type glutamate receptors--nonselective cation channels mediating fast excitatory transmission in the CNS. *EXS* **66**: 61-76.

Jones MV and Westbrook GL (1995) Desensitized states prolong GABA$_A$ channel responses to brief agonist pulses. *Neuron* **15**: 181-191.

Jones MV and Westbrook GL (1996) The impact of receptor desensitization on fast synaptic transmission. *Trends Neurosci* **19**: 96-101.

Katz B and Thesleff S (1957) A study of the desensitization produced by acetylcholine at the motor end-plate. *J Physiol* **138**:63-80.

Krishtal OA, Marchenko SM and Obukhov AG (1988) Cationic channels activated by extracellular ATP in rat sensory neurons. *Neuroscience* **27**: 995-1000.

Kuzmin AI, Lakomkin VL, Kapelko VI and Vassort G (1998) Interstitial ATP level and degradation in control and postmyocardial infracted rats. *Am J Physiol* **275**: C766-C771.

Lazarowski ER, Boucher RC and Harden TK (2003) Mechanisms of release of nucleotides and integration of their action as P2X- and P2Y-receptor activating molecules. *Mol Pharmacol* **64**: 785-795.

Mike A, Castro NG and Albuquerque EX (2000) Choline and acetylcholine have similar kinetic properties of activation and desensitization on the $\alpha_7$ nicotinic receptors in rat hippocampal neurons. *Brain Res* **882**:155-168.

Nicke A, Baumert HG, Rettinger J, Eichele A, Lambrecht G, Mutschler E and
Schmalzing G (1998) P2X$_1$ and P2X$_3$ receptors form stable trimers: a novel
structural motif of ligand-gated ion channels. *EMBO* **17**: 3016-3028.

Nishiyama A, Majid DS, Taher KA, Miyatake A and Navar LG (2000) Relation
between renal interstitial ATP concentrations and autoregulation-mediated
changes in renal vascular resistance. *Circ Res* **86**: 656-662.

North RA (2002) Molecular physiology of P2X receptors. *Physiol Rev* **82**: 1013-
1067.

North RA. (2004) P2X$_3$ receptors and peripheral pain mechanisms. *J Physiol*
**554**:301-308.

Paradiso KG and Steinbach JH (2003) Nicotine is highly effective at producing
desensitization of rat $\alpha_4\beta_2$ neuronal nicotinic receptors. *J Physiol* **553**: 857-
871.

Patneau DK and Mayer ML (1991) Kinetic analysis of interactions between
kainate and AMPA: evidence for activation of a single receptor in mouse
hippocampal neurons. *Neuron* **6**: 785-798.

Phillis JW, O'Regan MH and Perkins LM (1993) Adenosine 5'-triphosphate
release from the normoxic and hypoxic in vivo rat cerebral cortex. *Neurosci
Lett* **151**: 94-96.

Pratt EB, Brink TS, Bergson P, Voigt MM and Cook SP (2005) Use-dependent
inhibition of P2X$_3$ receptors by nanomolar agonist. *J Neurosci* **25**: 7359-7365.

Raman IM and Trussell LO (1995) The mechanism of alpha-amino-3-hydroxy-5-methyl-4-isoxazolepropionate receptor desensitization after removal of glutamate. *Biophys J* **68**: 137-146.

Rang HP and Ritter JM (1969) A new kind of drug antagonism: evidence that agonists cause a molecular change in acetylcholine receptors. *Mol Pharmacol* **5**: 394-411.

Rang HP and Ritter JM (1970a) On the mechanism of desensitization at cholinergic receptors. *Mol Pharmacol* **6**: 357-382.

Rang HP and Ritter JM (1970b) The relationship between desensitization and the metaphilic effect at cholinergic receptors. *Mol Pharmacol* **6**: 383-390.

Reitstetter R, Lukas RJ and Gruener R (1999) Dependence of nicotinic acetylcholine receptor recovery from desensitization on the duration of agonist exposure. *J Pharmacol Exp Ther* **289**: 656-660.

Rettinger J and Schmalzing G (2003) Activation and desensitization of the recombinant $P2X_1$ receptor at nanomolar ATP concentrations. *J Gen Physiol* **121**: 451-461.

Skorinkin A, Nistri A and Giniatullin R (2003) Bimodal action of protons on ATP currents of rat PC12 cells. *Gen Physiol* **122**: 33-44.

Sokolova E, Nistri A and Giniatullin R (2001) Negative cross-talk between anionic $GABA_A$ and cationic P2X ionotropic receptors of rat dorsal root ganglion neurons. *Journal of Neuroscience* **21**: 4958-4968.

Sokolova E, Skorinkin A, Fabbretti E, Masten L, Nistri A and Giniatullin R (2004) Agonist-dependence of recovery from desensitization of $P2X_3$ receptors

provides a novel and sensitive approach for their rapid up or downregulation.
*Br J Pharmacol* **141**: 1048-1058.

Souslova V, Cesare P, Ding Y, Akopian AN, Stanfa I, Suzuki R, Carpenter K, Dickenson A, Boyce S, Hill R, Nebenuis-Osthuizen D, Smith AJ, Kidd EJ and Wood JN (2000) Warm-coding deficits and aberrant inflammatory pain in mice lacking P2X$_3$ receptors. *Nature* **407**: 1015-1017.

**Footnotes page**

*These authors contributed equally to the study

**Legends**

**Scheme 1**

Cyclic model for P2X$_3$ operation, where R is the receptor resting state, A the agonist, R$^o$ the activated receptor, D$_f$ is a rapidly-developing desensitized state (Paradiso and Steinbach, 2003), while slower-occurring desensitized states are denoted with D. Lower case letters apposed to the arrows indicate the corresponding reaction rate constants.

**Figure 1.** Agonist activity on P2X$_3$ receptors. A, example of responses elicited by β,γ-meATP, α,β-meATP, ATP or 2-Me-SATP (all applied at 10 µM concentration) on the same rat DRG neuron. Note differential decay of currents. B, plots of current amplitude (as % of maximum for each agonist) versus log agonist concentration (5-10 rat cells). C, plots of log half-time (t$_{1/2}$) values of current decay following application of different agonists versus log agonist concentration. Datapoints are from 5-12 rat cells.

**Figure 2.** Recovery from desensitization depends on the type of the agonist. Plots of current amplitude induced by a test pulse of agonist after various intervals from the first test pulse of the same. Agonists were applied at equieffective concentrations: 2-Me-SATP (1 µM), β,γ-meATP (100 µM), α,β-meATP (10 µM) and ATP (10 µM). Data are from 4-10 rat DRG cells.

**Figure 3.** HAD modulates responses of rat P2X$_3$ receptors. A, example of protocol to induce HAD, whereby 10 nM $\alpha,\beta$-meATP is applied for 90 s prior to a test pulse of 10 μM ATP. While 10 nM $\alpha,\beta$-meATP has no detectable effect per se, it strongly inhibits the response to ATP. B, by using a similar protocol with 10 nM 2-Me-SATP, complete suppression of the test response to ATP is apparent. C, plot of current amplitude induced by a test pulse of 10 μM ATP after application (variable time; abscissa) of 10 nM ATP. Note that ~90 % inhibition of test responses is reached at 90 s exposure to 10 nM ATP. Data are from 4-5 rat cells. D, plots of current amplitude induced by a test pulse of 10 μM ATP after 90 s application of various concentrations (log scale; abscissa) of the agonists as indicated. Note differential potency to inhibit ATP currents. Data are from 4-7 rat cells.

**Figure 4.** Intensity of HAD depends on timing of nanomolar agonist application. A, example of inhibition of test responses (mouse TG neuron) to pulses of 100 μM $\beta,\gamma$-meATP (applied for 2 s once every 2 min) by 10 nM ATP administered for 60 s immediately after a test pulse. B, when the protocol is repeated by applying 10 nM ATP 60 s prior to the next test pulse, the current response is also inhibited, though less than before. Data are from a representative mouse TG neuron. C, D, plots of current amplitude (as % of control response) following 10 nM ATP applied (see shaded areas) at early or late times during the test pulse series. Data are from mouse TG neurons (n=6) or rat DRG neurons (n=6). E, depressant action of 10 nM ATP applied for 30 s immediately after test pulse of 5
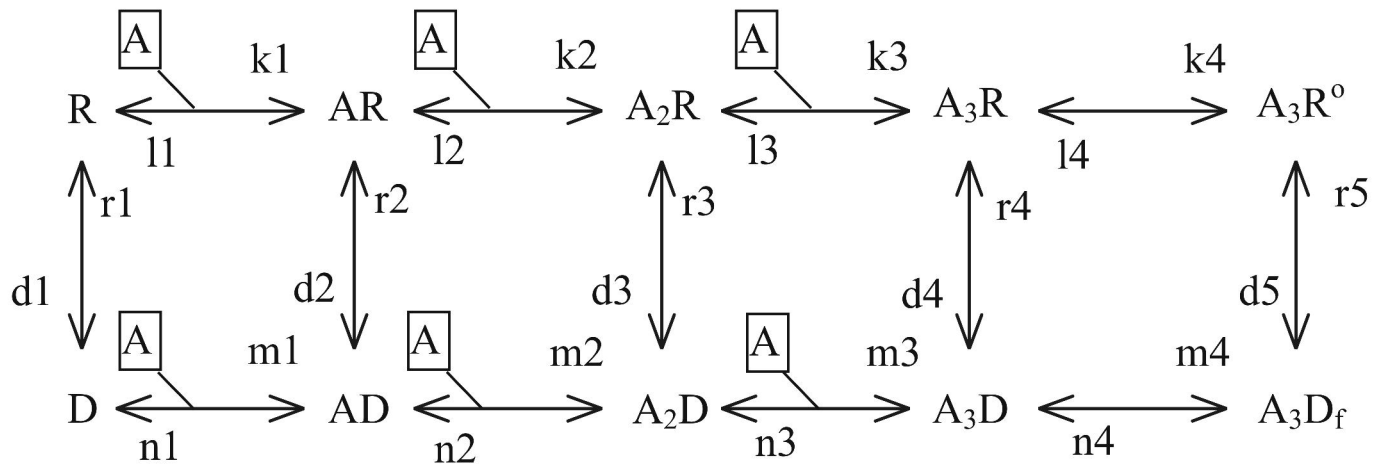
μM β,γ-meATP (early application – top panels) or after 30 s wash (late application

– bottom panels) to rat DRG neuron. F, histograms of current amplitude evoked

by a test pulse of 5 μM β,γ-meATP after early or late conditioning with 10 nM

ATP. Data (n=6) are expressed as % of preceding (non-conditioned) response.

*=P<0.05.

**Figure 5.** Kinetic model of P2X$_3$ receptor closely reproduces experimental

observations. A, theoretical log dose response curves for the indicated agonists

are very similar to the experimental ones (Fig. 1B). Inset shows simulated ATP

current with very similar shape to experimental one (Fig. 1A). B, plots of log half-

time (t$_{1/2}$) values of theoretical current decay following application of different

agonists versus log agonist concentration (compare with Fig. 1C). C, differential

timecourse for recovery from desensitization after various agonist applications.

Agonist doses and protocols are simulated like the experimental ones of Fig. 2.

D, plots of amplitude of theoretical current induced by a test pulse of 10 μM ATP

after 90 s application of various concentrations of the agonists as indicated. Note

differential agonist potency to inhibit ATP currents in agreement with data of Fig.

3D. E, F plots of theoretical current amplitude (as % of control response)

following simulation of 10 nM ATP application (see shaded areas) at early or late

times during the series of test pulses (100 μM β,γ-meATP; applied for 2 s once

every 2 min). For comparison with experimental data, see Fig. 4 C,D.
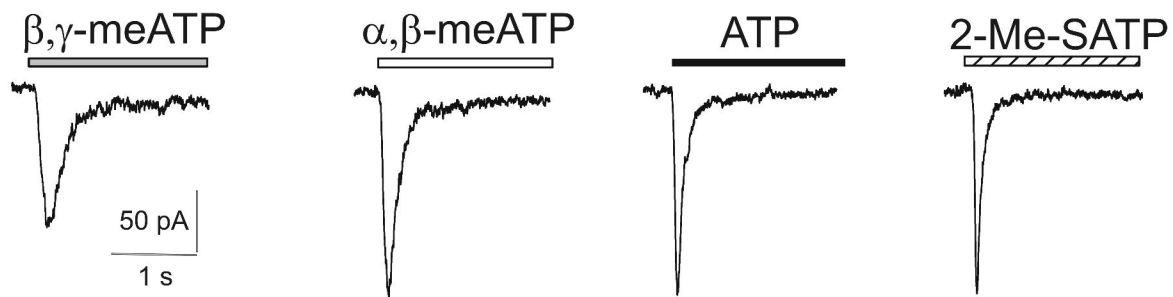
**Figure 6.** Simulated currents evoked by ATP in the presence or the absence of

HAD. Left, halfmaximal concentration of ATP (1 µM) generates theoretical responses identical in peak and timecourse regardless of the presence of HAD. Right, a near-threshold concentration of ATP (100 nM) evokes a simulated response of smaller amplitude (scaled, for the sake of comparison, to the larger response) the peak of which is not affected by HAD. Current decay is, however, accelerated in the presence of HAD.
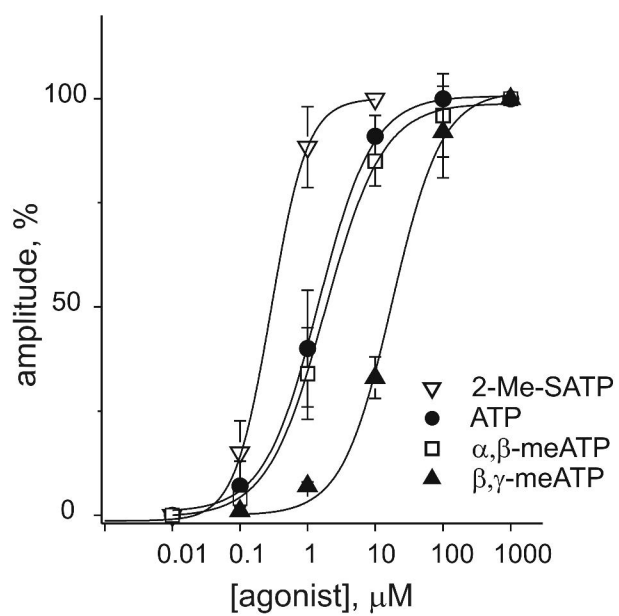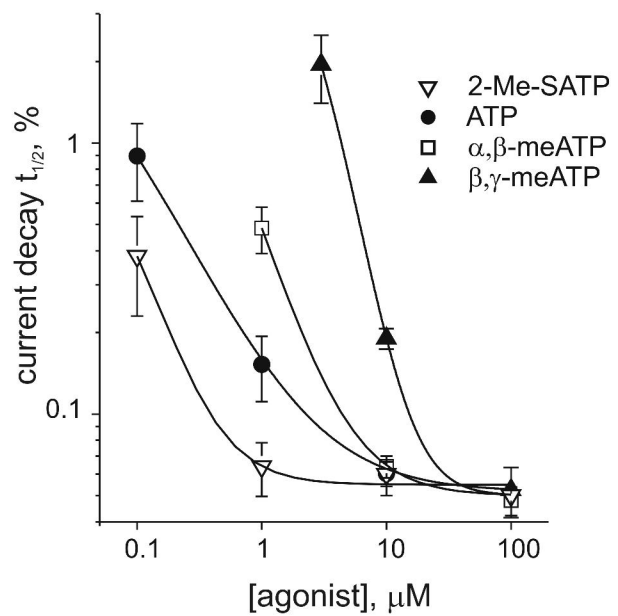
Scheme 1

Fig1

A


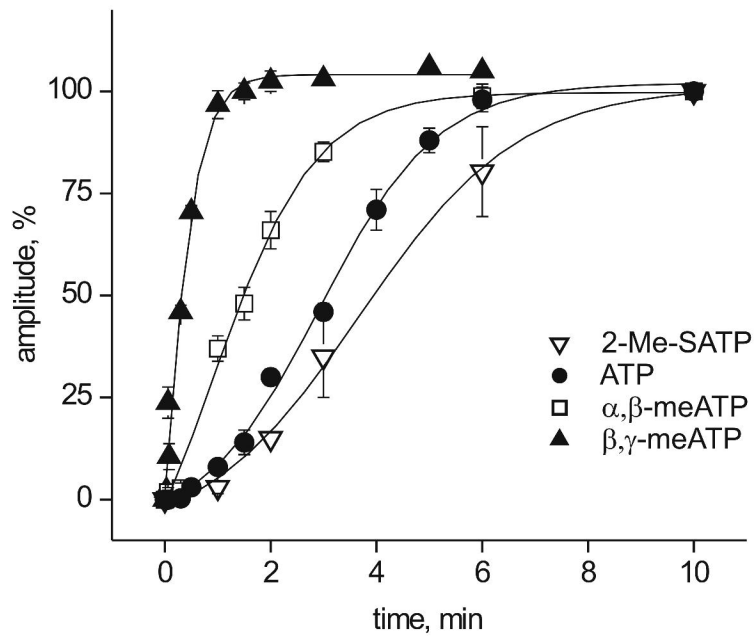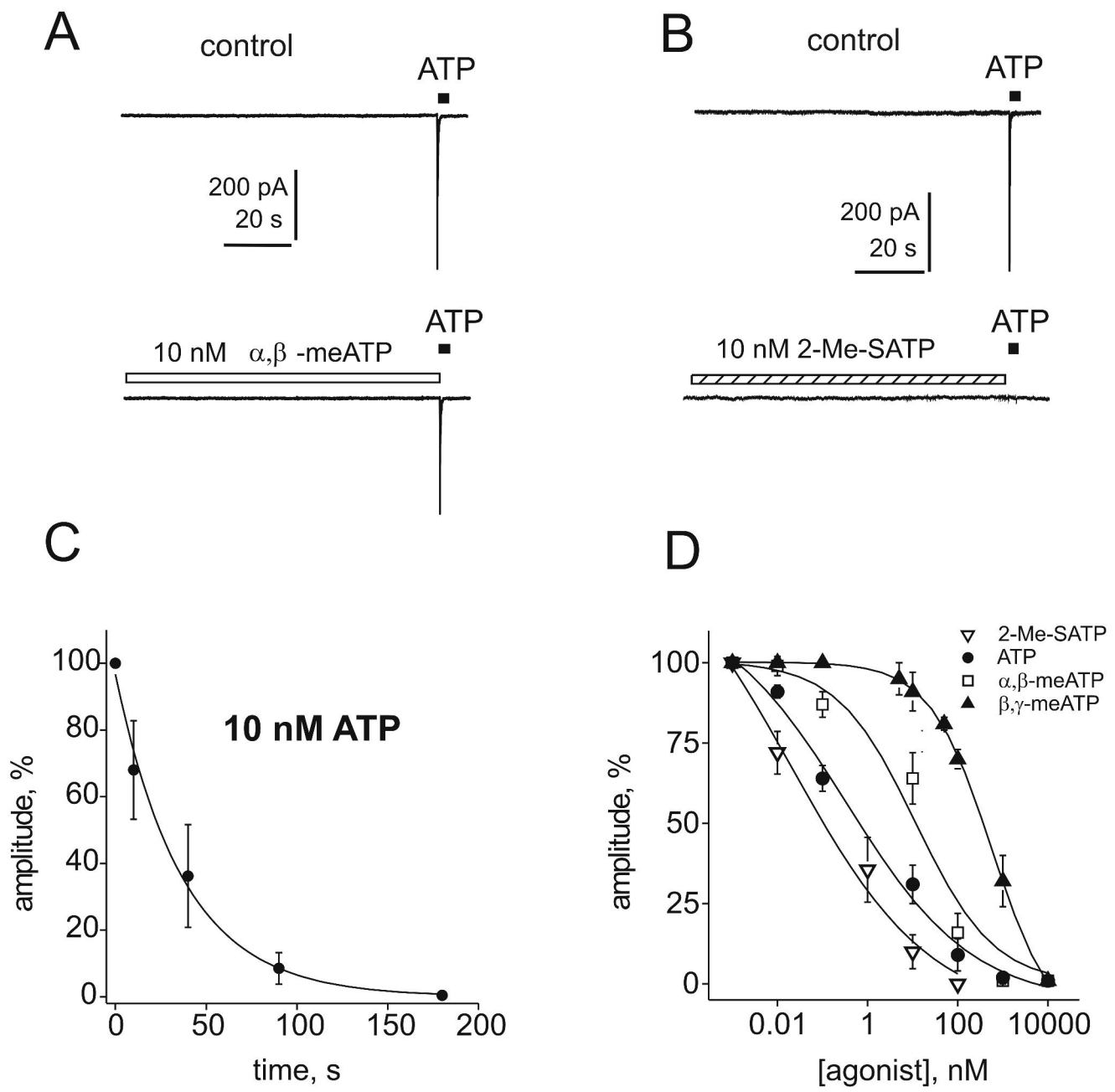
β,γ-meATP    α,β-meATP    ATP    2-Me-SATP

50 pA

1 s

B



amplitude, %

2-Me-SATP
ATP
α,β-meATP
β,γ-meATP

[agonist], μM

C



current decay t_{1/2}, %

2-Me-SATP
ATP
α,β-meATP
β,γ-meATP

[agonist], μM

Fig 2

Fig 3

Fig 4

Fig 5

Fig 6

1 μM ATP

100 nM ATP

+/- HAD

+HAD

-HAD

0.5 s | 0.05

2 s | 0.001